

Phase transformations and ordering in polyacetylene

L. W. Shacklette and J. E. Toth

Corporate Technology, Allied Corporation, Morristown, New Jersey 07960

(Received 17 May 1985)

Donor and acceptor complexes of polyacetylene containing the counterions K^+ , Na^+ , and PF_6^- have been investigated by electrochemical methods. First-order structural phase transformations as well as counterion-ordering transitions within structural phases have been identified for alkali-metal complexes of polyacetylene. The conductivities of the complexes exhibit relative maxima at the compositions of ordered phases. Ordered phases of $CHNa_y$ have been identified at compositions $y=0.0667$, 0.0833 , and 0.111 ; ordered phases of CHK_y are found at $y=0.0625$, 0.0833 , 0.125 , and 0.167 . Evidence is found for disproportionation into separate phases at intermediate doping levels, $0.003 < y < 0.06$. Conductivity σ at these intermediate levels is a strongly varying function of y . In this range, σ versus y data are well fitted by a variable-range-hopping model.

INTRODUCTION

Polyacetylene and poly(*p*-phenylene) are conjugated polymers which can be prepared with a high degree of crystallinity (up to 90%). These polymers can be either oxidized or reduced to form highly conductive complexes.¹⁻³ Most previous studies have treated the oxidation or reduction process as *p*-type or *n*-type doping, which was presumed to occur randomly among and along polymer chains. Recently we have used both x-ray and electrochemical measurements to demonstrate the existence of discrete stoichiometric phases of the crystalline oxidized^{4,5} and reduced complexes.⁵⁻⁷

In this view, electrochemical doping is characterized as an ion-insertion process. Experimental evidence suggests that this ion insertion (doping) proceeds, not at random, but via a sequence of crystalline phases. These phases involve either layered or channel structures and invariably require considerable perturbation of the crystal structure of the pristine polymer. The degree of crystallinity of the complex varies according to the crystallinity of the starting polymer and the size of the inserted counterion.

In this paper we will consider the effects of phase separation and order on the physical properties of polyacetylene complexes. We will investigate how crystallinity affects ion insertion, and we will present data on the details of the structural evolution of polyacetylene during Na^+ and K^+ insertion and extraction. The implications of this structural model on the behavior of conductivity at low doping levels encompassing the transition from semi-conducting to metallic behavior will also be considered.

EXPERIMENTAL

The crystalline polyacetylene film was prepared by the standard Shirakawa technique.⁸ Crystallinity was estimated from the relative strength of x-ray lines from crystalline regions compared with that of the background due to amorphous regions. A crystallinity index was arbitrarily set to correspond to the percentage of material displaying a coherence length greater than 30 Å. On this

basis, a typical unoriented film had a crystallinity greater than 70%. A typical density was 0.4 g/cm^3 , and the thickness ranged from 75 to 100 μm . Significantly less-crystalline polyacetylene (crystallinity $\sim 30\%$) was prepared from a mixture of acetylene and 1-hexyne, again using the Shirakawa catalyst. The ratio of reactants was adjusted to produce a random copolymer of acetylene and 1-hexyne in the very approximate ratio of 9:1. This copolymer consists of a polyacetylene backbone (alternating single and double carbon-carbon bonds) which is substituted by a small number of butyl side groups ($-C_4H_9$). These bulky side groups inhibit the regular packing of polyacetylene chains and also probably interrupt the conjugation by forcing a twist in the backbone. The undoped films have a silver-green appearance and a fibrillar morphology.

Electrochemical doping of polyacetylene or its copolymer with 1-hexyne was accomplished by forming a contact between the films and an open mesh of either platinum or nickel, immersing the polymer in an electrolyte containing the desired counterion for the doped polymer, and applying the appropriate anodic or cathodic potential. A detailed description of the choice and preparation of solvents and electrolytes for cation insertion (*n* doping) is presented elsewhere.⁹ Acceptor doping in this work was carried out in an electrolyte of $0.5M \text{ NaPF}_6$ in benzonitrile. A counterelectrode reversible to sodium ions was employed in order to ensure that no degradation products were formed during PF_6^- insertion and extraction. Isomerization to *trans*-polyacetylene was accomplished by an initial insertion and extraction cycle. All data presented here were taken on a second or later cycle after isomerization was completed.

Measurements of potential versus composition were taken with a computer-controlled incremental-voltage-step (IVS) technique.¹⁰ The potential of the polymer electrode versus a separate reference was stepped in 10-, 25-, 50-, or 100-mV increments or decrements between preset voltage limits. The current after each voltage step was allowed to decay to a preset minimum typically corresponding to $25 \mu\text{A/cm}^2$. Once the minimum current was

reached, the circuit was opened for one minute and the potential of the polymer was recorded after this wait. A typical insertion and extraction cycle required 30 h to complete with the longest high-resolution cycles requiring up to 10 days.

The composition was determined in every case from the starting weight of the pristine polymer and the number of Coulombs passed during ion insertion or extraction. In this paper, we will use the notation $(\text{CHD}_y)_x$ for the polymer complex, where D is the counterion, y the ratio of the number of ions to carbon atoms (the doping level), and x the degree of polymerization.

In situ conductivity measurements were made in a specially designed glass cell in which the sample was held against a glass rod by two spring-loaded wires (voltage leads) and two spring-loaded sections of wire mesh (current leads). In order to ensure that near uniform doping levels were maintained, the four contacts were arranged on the rectangular sample so that no part of the polyacetylene was farther than 0.5 mm from a metal current collector. All four contacts to the polyacetylene were maintained at the same potential during doping. At the end of each voltage step (i.e., when the sample reached a near-equilibrium doping level at the given potential), the four contacts were separated from each other and connected to an ac constant-current source (10 or 100 μA rms, 87 Hz) and a lock-in amplifier for the conductivity measurement. In this configuration, the ionically conducting electrolyte is in parallel with the electronically conducting sample. The parallel resistance of the ionic liquid could be determined when the sample was insulating (undoped), and subsequent readings were corrected accordingly. This parallel-resistance correction imparts a degree of uncertainty in measurements of conductivity below about 10^{-1} to $10^{-2} \Omega^{-1} \text{cm}^{-1}$. This restriction still allows an accurate measure of conductivity over a range of 4 or 5 orders of magnitude.

RESULTS AND DISCUSSION

The open-circuit potential measured in an electrochemical cell is related to the chemical potential of the polymer complex with respect to that of the reference electrode. Previous experiments¹¹ on polyacetylene with the IVS technique have demonstrated that the electrochemical behavior of polyacetylene at very low doping levels (less than about 1500 ppm) is dominated by the electronic structure of polyacetylene. Successful estimates of the band gap and even the energy of defect states within the gap have been made. Similar results have been obtained with other polymers.^{3,12} In the present work, we will demonstrate that at higher doping levels ($y > \sim 0.01$) structural effects dominate, and any description of polyacetylene complexes based solely on the electronic band structure of the pristine polymer breaks down.

We have already noted that alkali-metal-ion insertion in polyacetylene induces the formation of particular stoichiometric phases, which we denote $[(\text{C}_n\text{H}_n)_m M]_x$, where alkali-metal ions (M) are arranged in columns, m denotes the number of polymer chains per ion column, and n denotes the number of CH units along a given

chain, which corresponds to the average spacing of alkali-metal ions within their columns. If all columns are equivalent and all ion spacings are equal, then n will be an integer if the positioning of alkali-metal ions is commensurate with the backbone periodicity. In all cases the average spacing of alkali-metal ions within columns will be $n(1.24 \text{ \AA})$. The average doping level for the polyacetylene is $y = (nm)^{-1}$. We find experimentally that $3 \leq n \leq 5$ and $2 \leq m \leq 4$ when $M = \text{Na}^+$ or K^+ . The maximum average doping level for crystalline regions of polyacetylene inserted by Na^+ or K^+ is then $y = 0.167$.

One expects that structural phase transformations between different values of m will be discontinuous (first order) since these transformations involve considerable movement and rearrangement of polymer chains. In addition, there is also the possibility of the ordering of alkali-metal ions (and even order-disorder transitions) within the sublattice of available sites in each column or layer of columns. These possibilities are exactly analogous to those which have been demonstrated for a variety of two-dimensional layered intercalation compounds (see, for example, Refs. 13 and 14). One might be concerned, however, about the possible one dimensionality of our system since a basic theorem states that long-range order cannot exist in a one-dimensional system whose elements interact through finite-range forces.¹⁵ This theorem, however, will not apply to polyacetylene, since the imposition of finite conjugation length or a small amount of coupling with neighboring metal columns will allow the appearance of long-range order. In any case, the question of the existence of long-range order among counterions in dilute phases ($n > 3$, $m > 2$) is left open since long-range order is not a necessary requirement for the appearance of phase transitions. Thus, many of the effects to be presented here could be explained only on the basis of short-range order (i.e., the local clustering of counterions in a regular array). Coherence lengths inferred from x-ray measurements on alkali-metal complexes of polyacetylene (K, Rb, Na) have been reported to be 60 to 100 \AA perpendicular

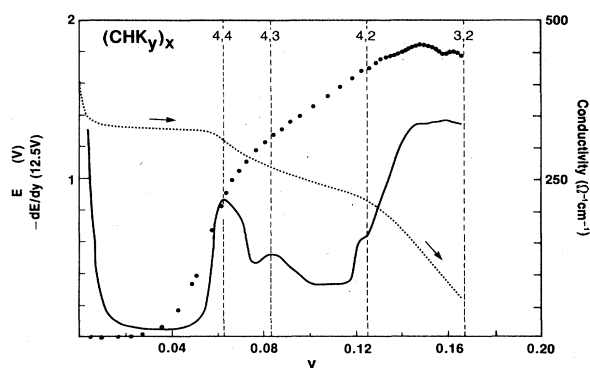


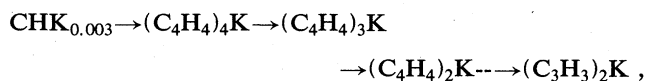
FIG. 1. K^+ -ion insertion showing the open-circuit potential E versus composition y (dotted line), its derivative $-dE/dy$ vs y (solid line), and the electrical conductivity σ vs y (points). Vertical dashed lines with n, m values shown indicate the compositions $(\text{C}_4\text{H}_4)_4\text{K}$, $(\text{C}_4\text{H}_4)_3\text{K}$, $(\text{C}_4\text{H}_4)_2\text{K}$, and $(\text{C}_3\text{H}_3)_2\text{K}$. The composition data are scaled by a factor of 1.07 to fit the peak at $(\text{C}_4\text{H}_4)_3\text{K}$.

lar to the chain direction and $>45 \text{ \AA}$ along the chain.¹⁶

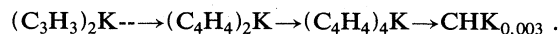
Electrochemical and conductivity data for potassium insertion and extraction in polyacetylene are presented in Figs. 1 and 2. Generally not all of the polyacetylene in a given sample is crystalline, nor will it all necessarily be in electrical contact with all the other parts of the sample; therefore, we have chosen in this paper to correct the apparent doping level y to a value more equal to the actual doping level in crystalline regions. The value of y suggested by x-ray data is invariably higher than the apparent value.⁶ To a first approximation we assume that a simple multiplicative correction is appropriate. The value of this correction factor (generally ranging from 1.03 to 1.12) is chosen to fix a prominent feature of the electrochemical behavior to a particular nearby theoretical composition. In Fig. 1 the composition axis was scaled (correction factor of 1.07) to allow the peak in $-dE/dy$ near $y=0.08$ to fall exactly at the theoretical composition for a phase ($m=3$) observed in x-ray diffraction measurements, $(C_4H_4)_3K$ ($y=0.0833$). The other peaks then fall where they may. In Fig. 2 the curves were fitted to the peak at the composition $(C_4H_4)_2K$ ($y=0.125$) by adjusting the composition values by a factor of 1.105. The larger correction factor for ion extraction reflects a slight inefficiency of the electrochemical doping process most likely brought about by chemical side reactions with impurities. The conductivity was measured on a similar sample of polyacetylene, but ion insertion and extraction was accomplished in a shorter period (~ 13 h per half-cycle) compared to that taken to obtain the high-resolution electrochemical potential data shown in Figs. 1 and 2 (5 days per half-cycle). The conductivity data were matched independently to the compositions $(C_4H_4)_3K$ (Fig. 1) and $(C_4H_4)_2K$ (Fig. 2) using lower-resolution $-dE/dy$ data collected on this sample during the conductivity measurement. Arguments for our association of maxima in $-dE/dy$ (i.e., minima in $-dy/dE$, the incremental capacity) with the compositions of ordered phases have been developed for intercalation in layered dichalcogenides.¹⁷⁻¹⁹ This idea, that maxima in $-dE/dy$ versus y correspond to ordered phases, is further

strengthened by the observation of similar relative maxima in the conductivity at corresponding values of y .

The combined evidence of conductivity and electrochemical potential measurements suggests that the structural evolution of crystalline polyacetylene during K^+ -ion insertion proceeds according to



and during K^+ -ion extraction according to



In Fig. 2 there are also two minor features (knees) on the peaks for the compositions $(C_4H_4)_2K$ and $(C_4H_4)_4K$, which suggests that during extraction the $m=2$ phase is retained until nearly $(C_5H_5)_2K$ and the $m=4$ phase until $(C_5H_5)_4K$. These phases are likely to be only metastable because of the long spacing between K^+ ions (6.20 \AA). In the above scheme, dashed arrows denote transitions to ordered composition within a particular phase (fixed m), and solid arrows denote first-order transitions between structural phases (change in m). Such changes in m are always accompanied by plateaus in the E -versus- y graph (minima in $-dE/dy$). Corresponding relative minima in the conductivity-versus- y graph reflect the increased disorder incurred during a structural phase transformation. X-ray diffraction studies and structure modeling^{6,7} give independent support for structures having compositions $(C_nH_n)_3K$ and $(C_nH_n)_2K$, that is, structures having three chains and two chains per column, respectively. An observed long spacing of 11.7 \AA suggests the possibility of structures having four or more chains per column, but complete structural models based on these x-ray data have not been developed.

Similar electrochemical and conductivity data are presented for Na^+ insertion and extraction in polyacetylene in Figs. 3 and 4. In this case the theoretical composition of $(C_4H_4)_3Na$ ($y=0.0833$) is used as a guide for establishing the scale correction for y for both insertion and extraction. The actual value of y in crystalline re-

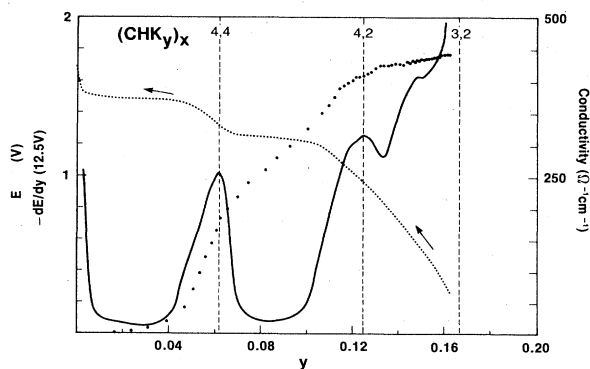


FIG. 2. K^+ -ion extraction showing E vs y (dotted line), $-dE/dy$ vs y (solid line), and σ vs y (points). Dashed lines with n,m values shown indicate the compositions $(C_3H_3)_2K$, $(C_4H_4)_2K$, and $(C_4H_4)_4K$. The composition data are scaled by a factor of 1.105 to fit at $(C_4H_4)_2K$.

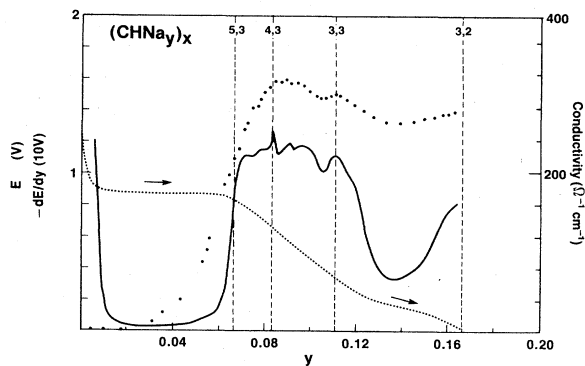


FIG. 3. Na^+ -ion insertion showing E vs y (dotted line), $-dE/dy$ vs y (solid line), and σ vs y (points). Dashed lines with n,m values shown indicate the compositions $(C_5H_5)_3Na$, $(C_4H_4)_3Na$, $(C_3H_3)_3Na$, and $(C_3H_3)_2Na$. The composition data are scaled by a factor of 1.050 to fit at $(C_4H_4)_3Na$.

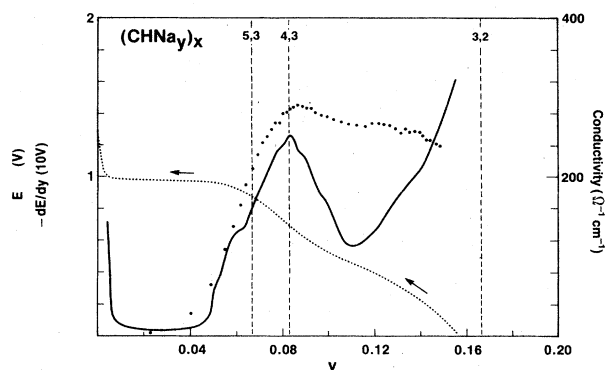
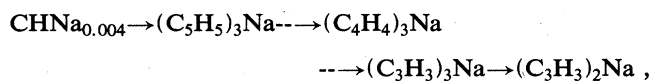
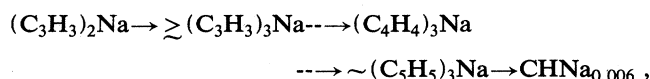


FIG. 4. Na⁺-ion extraction showing E vs y (dotted line), $-dE/dy$ vs y (solid line), and σ vs y (points). Dashed lines with n,m values shown indicate the compositions $(C_3H_3)_2Na$, $(C_4H_4)_3Na$, and $(C_5H_5)_3Na$. The composition data are scaled by a factor of 1.057 to fit at $(C_4H_4)_3Na$.

gions is again found to be slightly larger than the apparent average value of y . Notice that Na⁺-inserted polyacetylene exhibits even more pronounced maxima in conductivity near the compositions of ordered phases. The sequence of ordered phases with sodium is slightly different from that with potassium. The first ordered phase appears at a higher y value near $y=0.0667$. The experimental evidence suggests that m must be equal to or less than 3 for $(C_nH_n)_mNa$, i.e., no more than three chains per column of sodium. This difference in behavior most likely results from the smaller size of the sodium ion which is not large enough to fill the channels created by a tetragonal arrangement of chains.¹⁶ Nevertheless, ordering does have a pronounced effect on the properties of sodium complexes of polyacetylene. The suggested sequence of major ordered phases during ion insertion is



while for extraction it is



where, again, solid lines indicate major structural transformations (changes in m) and dashed lines indicate transitions to ordered compositions (preferred values of n) within a particular structural phase.

An expanded view of $-dE/dy$ is presented in Fig. 5, where the data have been adjusted to fit at $(C_4H_4)_3Na$ as in Figs. 3 and 4. X-ray data for the phase having $m=3$ with Na⁺ counterions are not consistent with a tetragonal arrangement of polyacetylene chains, a difference which, as already mentioned, undoubtedly results from the small size of the sodium ions. Unfortunately, the x-ray data presently available do not provide enough information to develop a detailed model of the actual structure. The electrochemical data, however, provide strong support for the existence of a structural phase having a stoichiometry of three chains per column of sodium ions. The nearly linear

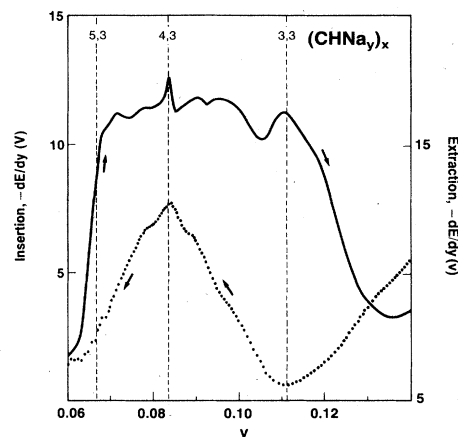


FIG. 5. Na⁺-ion insertion (solid line) and extraction (dotted line). The composition values are scaled to fit at $(C_4H_4)_3Na$. The insertion curve represents the average of three samples, the extraction curve the average of two. Dashed vertical lines with m,n values shown are at compositions $(C_3H_3)_3Na$, $(C_4H_4)_3Na$, and $(C_3H_3)_3Na$.

behavior of the potential in Fig. 3 from $y \cong 0.07$ to $y \cong 0.11$ suggests that a single structural phase persists over this range. Such an extensive composition range can be fitted by a model based on three chains per column where n,m may vary from 5,3 ($y=0.0667$) to 3,3 ($y=0.111$). An alternate possibility which cannot be entirely ruled out is that the peak in $-dE/dy$ near $y=0.0833$ (Fig. 5) is associated with a phase having four chains per column (i.e., $n,m=3,4$ rather than 4,3) as is the case with K⁺ (Fig. 1). The weak minimum near $y=0.105$ would then be associated with a phase transformation from four chains per column to three chains per column.

In either case, evidence can also be found for noninteger values of n . Because of the strong interaction between unscreened positive ions in a single column, it is not likely that noninteger values of n result from a regular distribution of columns having different uniform spacings. Rather, it is more likely that each column possesses a regular array of different commensurate spacings. For example, a periodic array of $n=4$ spacings and $n=3$ spacings in a given column will give $n=3.67$ and $n=3.33$ for a ratio of four and three spacings of 2:1 and 1:2, respectively. As discussed previously, it is likely that correlations of spacings in neighboring columns also occur. The possible observation of noninteger values of n for sodium complexes prompts a return to the data for K⁺-inserted polyacetylene presented in Figs. 1 and 2, where one may note the presence of weak features in $-dE/dy$ at noninteger compositions corresponding to m,n values of 4.33,4; 3.67,4; 3.67,3; 3.67,2; and 3.33,2.

A high degree of uncertainty, nevertheless, remains concerning the proposed existence of ordered phases having noninteger values of n . Although every ordered phase should be associated with a maximum in $-dE/dy$, the converse is not true; that is, every relative maximum does not imply an ordered phase. As already mentioned,

several authors have used various lattice-gas models (which neglect electronic effects) to explain the observation of order-disorder transitions in layered intercalation compounds.¹⁷⁻¹⁹ Calculations on these compounds predict, and measurements support,¹³ the presence of maxima in $-dE/dy$ at the compositions of ordered phases surrounded on both sides by minima corresponding to the transitions between disordered and ordered phases as a function of y . These minima are not to be confused with the minima associated with changes in m . However, when a change in structural phase occurs near an ordering transition, the latter will be obscured by the former. In polyacetylene, there appear to be examples of both circumstances. For instance, the ordered compositions of $(C_4H_4)_3Na$ and $(C_3H_3)_3Na$ (Fig. 5) are both surrounded by nearly symmetric minima, although the minima on the high- y side of the latter composition is partly obscured by the nearby transition from the $m=3$ to the $m=2$ phase. The phases at compositions $(C_4H_4)_3K$, in Fig. 1, and $(C_4H_4)_2K$, in Fig. 2, also show evidence for nearly symmetric minima, which are again affected by nearby structural phase transitions.

One expects that the ordered phases possessing long-range order within a given structural phase may also exhibit order-disorder transitions as a function of temperature. Unfortunately, the range of temperature over which *in situ* measurements can be made is restricted by dopant diffusion at low temperature and electrolyte stability at high temperature. Nevertheless, we have made measurements of $-dE/dy$ versus y over a temperature range from 0°C to 75°C. Our observations support a general tendency for the amplitude of the variation in $-dE/dy$ near ordered compositions to decrease with increasing temperature as one expects for an ordered system approaching an order-disorder transition. As an example, the temperature dependence of the peak in $-dE/dy$ at the composition $(C_4H_4)_3Na$ can be seen in Fig. 6. Since the satellite minima corresponding to ordering are still

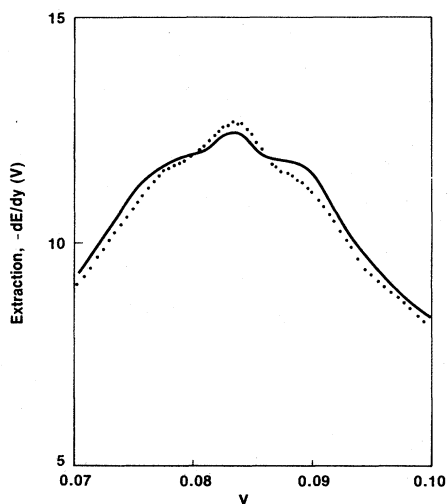


FIG. 6. Na^+ -ion extraction at 22°C (dotted curve) and 72°C (solid line). Data presented for both curves are the average of two samples.

present at 72°C, the critical temperature for any ordered phase having long-range order must be greater than this temperature. Alternatively, one may only be observing a continuous decrease in short-range order with increasing temperature.

Since the crystalline perfection of polyacetylene and other conducting polymers is very low in comparison with various inorganic intercalation compounds which have been previously studied, it is important to consider how the limited crystallinity of conducting polymers may influence the ordering effects which are described in this work. For instance, evidence for ordering within a structural phase becomes more distinct for samples which have been carefully prepared and handled and which presumably possess long conjugation lengths. On the other hand, even among amorphous polyacetylene complexes, plateaus in electrochemical potential as a function of composition are ubiquitous. As an illustration, consider the data in Fig. 7 for tetrabutylammonium-ion insertion and extraction in polyacetylene. This complex appears amorphous in x-ray diffraction measurements and yet still exhibits a relative (but weaker) plateau in the E -versus- y graph at low y values. This behavior is a consequence of the fact that even though the complex is amorphous, the pristine starting material is crystalline. During ion insertion the crystallinity is lowered and the polymer chains are separated and rearranged. The elastic energy necessary to accomplish this reorganization causes the transition from close-packed to separated chains to be first order, thereby causing the initial flattening of the electrochemical potential at low y . A similar effect has been predicted and found in other intercalation systems.²⁰ We may pursue these ideas further by considering the situation where the original polymer is substantially less crystalline. While it will still be necessary to separate chains to allow the insertion of counterions, there will be less cohesive energy to overcome in polymers of limited crystallinity. As a consequence, one expects to see less flattening of the E -versus- y curve at low y . In fact, we have been able to observe this effect in polyacetylene in several

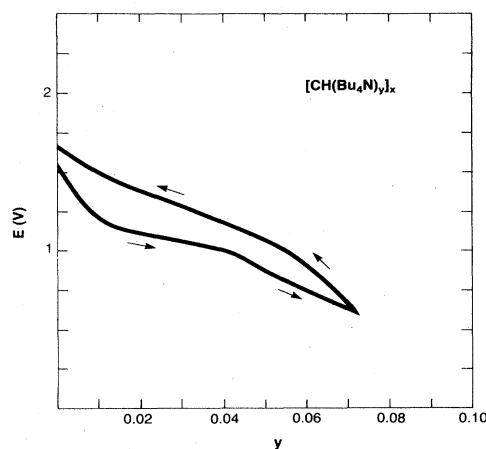


FIG. 7. Bu_4N^+ -ion insertion and extraction in polyacetylene. The potential E is measured with respect to a Na reference electrode.

ways. There are a variety of routes to low crystallinity or amorphous polyacetylene. Among these, we have chosen two which retain the fibrillar morphology of the highly crystalline polyacetylene studied here. Firstly, we have observed that repeated electrochemical cycling gradually destroys the crystallinity of polyacetylene. After several hundred insertion and extraction cycles, we have observed a general tendency for the first plateau to weaken or disappear, especially with Li^+ and also to a lesser extent with Na^+ or K^+ . Secondly, we have prepared a copolymer of acetylene and 1-hexyne which has bulky side groups (butyl) and which has decreasing crystallinity with increasing 1-hexyne content. This polymer may also be swelled by a variety of solvents. The solvent interaction which causes swelling further overcomes the cohesive energy of the polymer lattice. Results obtained with this solvent-swollen copolymer initially having 30% crystallinity are compared with those of crystalline unswollen polyacetylene in Fig. 8, where Li^+ insertion and extraction are carried out in an electrolyte of lithium tetrabutylborate in 2-methyltetrahydrofuran. The initial plateau at low y is absent in the copolymer due to the combined effects of solvent swelling and lower crystallinity. The plateau seen at low voltage and higher values of y may be due to a conjugation-length distribution which favors short lengths in the more disordered copolymer. Raman studies²¹ on electrochemically prepared potassium complexes of polyacetylene have shown that short chain segments (fewer than seven double bonds) become doped only at potentials near that of potassium metal ($E < 0.5$ V with respect to a potassium reference).

Results obtained with sodium-ion insertion and extraction also support the tendency toward less distinct plateaus for the copolymer; however, the difference is significantly less dramatic. The similarity in behavior of the copolymer with crystalline polyacetylene partly stems from the fact that there is less tendency with Na^+ to coinsert solvent,⁹ and, therefore, for the polymer to become grossly swollen. This similarity in behavior between poly-

mers with significantly different conjugation lengths also adds credence to the possibility that the ordering effects described in this work require only short-range order.

While the consideration of elastic energy leads to a general flattening in E versus y , complete disproportionation into separate phases will cause $-dE/dy$ to become identically zero in the absence of kinetic limitations. This behavior is observed experimentally for both Na^+ and K^+ insertion in polyacetylene (Figs. 1–4). The evidence suggests that polyacetylene is separated at low y values into phases having the approximate compositions $y \leq 0.004$ and $y = 0.06$ (highly conducting). As has been previously suggested for iodine-doped polyacetylene,²² this phase separation may produce percolation behavior. Evidence has accumulated that a simple model of metal particles embedded in an insulating matrix does not explain the details of the behavior of iodine-doped polyacetylene.²³ More recently, evidence has been found that iodine aggregates on a molecular level into planar arrays, and a conducting-sheet model has been proposed.⁵ Since in the present work we have been able to obtain a relatively large number of points of conductivity against accurately known y values, it is worthwhile to consider the expected behavior of conductivity in polyacetylene at low y values.

Within a percolation model, the conductivity σ near the percolation limit is expected to behave according to the relation

$$\sigma(P) \propto (P - P_c)^t, \quad (1)$$

where P is the probability of a conducting link, P_c is the critical probability, and t is the critical exponent.²⁴ For a system having conducting and insulating components which are randomly distributed, P may be associated with the concentration of the conducting species, and P_c with the concentration necessary for the formation of an infinite cluster of the conducting species. In our problem, we identify P and P_c with y and y_c .

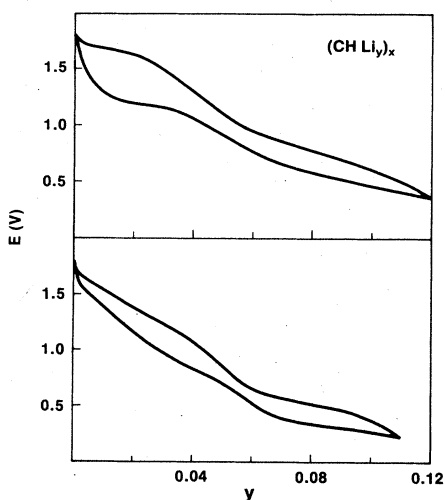


FIG. 8. Li^+ -ion insertion in polyacetylene (top curve) and in a copolymer of acetylene and 1-hexyne (bottom curve).

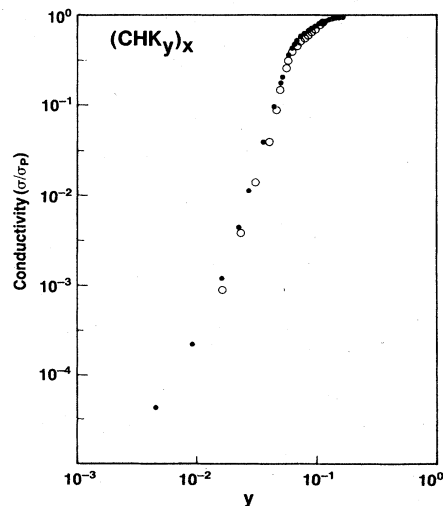


FIG. 9. Conductivity versus composition for K^+ insertion (solid circles) and extraction (open circles). The maximum conductivity (σ_p) for this sample equaled $487 \Omega^{-1} \text{cm}^{-1}$.

Our measurements of conductivity in the region $y < 0.06$, shown in Fig. 9, for K^+ insertion and extraction, indicate a very rapid rise in conductivity over the range $0.01 < y < 0.05$. The log-log plot of Fig. 9 suggests a power-law dependence of conductivity on y within this range, i.e., $\sigma \propto (y - y_c)^t$, where $t \cong 4.5$. Similar values of t are found for other counterions, i.e., Na^+ and PF_6^- . In all cases, the best fit to Eq. (1) is found for very low values of y_c (generally, $0 \leq y_c \leq 0.004$). Mathis and Francois²⁵ also observe a rapid rise in two-probe conductivity with y for *in situ* measurements on samples chemically doped with Li and Na. They also obtain an exponent t near 5 but observe no ordering effects at high doping levels.

Scaling theory²⁴ predicts that t should have a universal (i.e., lattice-independent) value in the range 1.6–2.0 for a three-dimensional lattice. The value of t observed in polyacetylene is obviously much greater than the universal value. There are, however, many features of this experiment and of polyacetylene itself which will likely lead to nonuniversal behavior. Unfortunately, we have little direct information on the size, shape, or distribution of the conducting phase in polyacetylene. Raman spectroscopy on potassium-doped samples indicates that long chains are the first to be doped.²¹ These long chains undoubtedly lie within crystalline regions. The tendency to open and then fill channels during ion insertion probably leads to cigar-shaped conducting regions. The application of percolation theory requires random spacing and orientation of these conducting regions. A theoretical treatment of a two-dimensional collection of "sticks" has shown the importance of this random orientation.²⁶ In our case, orientation is not random either within or between crystalline regions. Also, since doping is performed electrochemically, one must consider the fact that doping of a particular site is regulated by the transport to that site of both ions from the electrolyte and electrons (or holes) from the current collector. Thus, a tendency to form contiguous networks of conductive regions during doping is enhanced. During dedoping, however, these networks are expected to be selectively broken down. Such processes should give rise to marked hysteresis in conductivity as a function of composition during doping and dedoping. Our data, however, exhibit only a small hysteresis; thus, the rate of doping is sufficiently low and the inherent conductivity of undoped polyacetylene is sufficiently high to allow a relatively uniform macroscopic distribution of conductive regions.

Even though universal behavior is not observed, some type of percolation behavior is expected. It is likely that at low values of y , charge carriers will have to hop or tunnel between regions of high conductivity. It is not possible to determine with the present data whether these regions are to be associated with given sections of polymer chains, whole polymer chains, or groups of chains over which local order extends. Such problems can be approached with a hopping model derived from simple physical considerations²⁷ or more elegantly from a percolation treatment.²⁸ In our case, we expect charge carriers to be localized either by a physical barrier (the boundary between phases of high and low conductivity),

by disorder, or by a combination of both. In all cases, the conductivity will depend on the probability P of a hop, which may in the low-field limit be expressed as

$$P = \nu_0 \exp(-2\alpha R - W/kT), \quad (2)$$

where α^{-1} is a length associated with the spatial extent of the wave functions describing the localized carriers, R is the hopping distance, W is the energy difference between localized states, and ν_0 is the hopping attempt frequency. This frequency (ν_0) is usually associated with the average phonon frequency (ν_{ph}), but may in some instances be much larger than ν_{ph} .²⁹ If $2\alpha R \gg W/kT$, then hopping to nearest-neighbor sites will predominate, since the probability of a hop will be maximum for minimum R . When $2\alpha R \sim W/kT$, variable-range hopping (VRH) occurs. The VRH model has been previously applied to polyacetylene chemically doped with iodine. This model seems to give a reasonable description of the behavior of conductivity as a function of temperature³⁰ and optical density.³¹ With iodine, the actual doping level y is difficult to determine accurately since the counterion may be a variety of polyiodides, $(I)_{2n}I^-$. For this reason Kanicki *et al.*³¹ were forced to resort to optical density instead of y as a determination of the concentration of the conductive polyacetylene complex. In the present work, however, the value of y is accurately known from the amount of charge passed on doping and/or dedoping.

The VRH expression²⁷ for the dc conductivity is derived from the Kubo-Greenwood formula assuming that only carriers within kT of the Fermi energy contribute to the conduction. The expression has the form

$$\sigma = e^2 \nu_0 N_F R^2 \exp(-2\alpha R - W/kT), \quad (3)$$

where N_F is the density of localized states at the Fermi level expressed as states per unit energy per unit volume, and ν_0 , R , α , and W are as previously defined. If the probability of a hop in three dimensions is assumed to be spherically symmetric, then R is proportional to the inverse cube root of the carrier density, which is in turn proportional to y . If the conductive regions are indeed elongated (as with cigar-shaped domains or polymer chains themselves), the effect will be to reduce the dimensionality of the problem.

Now let us consider the behavior of the relative conductivity for the two-phase region which exists for $y < \sim 0.06$. We define σ_0 as the bulk conductivity at the single-phase composition y_0 , which occurs near the end of the first plateau. At all compositions $y < y_0$, the polymer is assumed to be divided between a high-conductivity phase having a local composition approximating y_0 and a low-conductivity phase having $y \cong 0.004$. At any composition $0.004 < y < y_0$, the average density of states may be expressed as $N_F = N_0 y / y_0$. In a three-dimensional treatment, the distance of an average hop R is related to the density of charge carriers n through the expression $nR^3 = q$, where q is a numerical constant of order unity. Estimates^{27,28} of q range from $3/(4\pi)$ to 4. We shall consider $nR^3 = 1$ from which follows

$$R = [13/(yN_0\rho)]^{1/3} = Ay^{-1/3},$$

where ρ is bulk density (~ 1.2 g/cm³), and N_A is Avagadro's number, which gives $A = 2.62$ Å. Assuming that W is not a function of y_0 , leads to

$$\sigma/\sigma_0 = (y/y_0)^{1/3} \exp\{-2\alpha A y_0^{-1/3} [(y/y_0)^{-1/3} - 1]\}. \quad (4)$$

We may write

$$\ln[(\sigma/\sigma_0)(y/y_0)^{-1/3}] = -2\alpha A y_0^{-1/3} (y/y_0)^{-1/3} + 2\alpha A y_0^{-1/3}. \quad (5)$$

This expression is similar to that obtained by Kanicki,³¹ where in the present case, y/y_0 has replaced optical density. In Fig. 10, a reasonably good fit to Eq. (5) is found over the range $0.01 < y < 0.06$ for the three counterions investigated, Na⁺ ($\sigma_0 = 220$ Ω⁻¹cm⁻¹, $y_0 = 0.0667$), K⁺ ($\sigma_0 = 225$ Ω⁻¹cm⁻¹, $y_0 = 0.0625$), PF₆⁻ ($\sigma_0 = 490$ Ω⁻¹cm⁻¹, $y_0 = 0.051$). As mentioned earlier, considerable uncertainty accompanies low conductivities obtained at low doping levels, since the effect of the correction for the parallel conductance of the electrolyte becomes significant. Such considerations may contribute to the deviation observed for $y < 0.01$ in Fig. 10. Equation (5) relates the slope of the curve in Fig. 10 to the decay length of the wave function describing the localized charge carriers. One obtains $\alpha^{-1} = 1.3$ to 1.7 Å and a minimum hopping distance of 6 to 7 Å for the three counterions investigated.

If one now wishes to consider the effects of an elongated geometry for the conductive regions, one may simply redefine the relation between hopping distance R and carrier density n . We will consider the relation to be approximately $nLR^2 = 1$, where L is the average length of a conductive domain. Making the assumption that L is not a function of y effectively reduces the model to two dimensions. Our relation between relative conductivity σ/σ_0 and relative composition y/y_0 now becomes

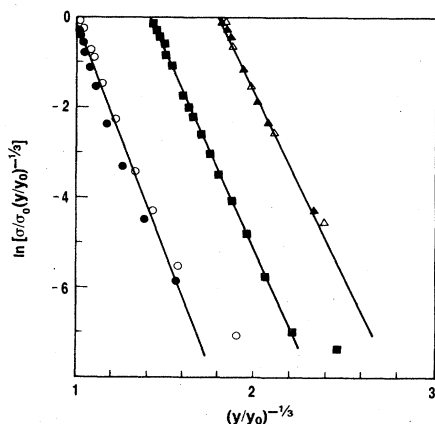


FIG. 10. Conductivity upon insertion (open symbols) and extraction (solid symbols) as a function of composition for a spherically symmetric three-dimensional hopping model. Polyacetylene complexes contain the counterions K⁺ (circles), Na⁺ (triangles), and PF₆⁻ (squares). The abscissae of the data for each ion are successively offset by 0.4 for clarity.

$$\sigma/\sigma_0 = \exp\{-2\alpha A^{3/2}(Ly_0)^{-1/2}[(y/y_0)^{-1/2} - 1]\},$$

or

$$\ln(\sigma/\sigma_0) = -2\alpha A^{3/2}(Ly_0)^{-1/2}(y/y_0)^{-1/2} + 2\alpha A^{3/2}(Ly_0)^{-1/2}. \quad (6)$$

As can be seen from Fig. 11, the data in the range $0.01 < y < 0.06$ fit this relation only slightly less well than Eq. (5). X-ray coherence lengths for most crystalline phases as well as estimates of typical conjugation lengths suggest that $L < 100$ Å. If one takes $L = 50$ Å, the slopes of Fig. 11 give $\alpha^{-1} = 0.75$ to 1 Å and a minimum hopping distance of 2 to 3 Å. These values of α^{-1} and R as well as those obtained in our spherically symmetric treatment are generally small compared to those found in amorphous semiconductors.³² The present results suggest that charge carriers are strongly localized in the chains surrounding a column of inserted ions, as has been predicted on the basis of calculations of Madelung energies for high-stage polyacetylene-iodine complexes.⁵

CONCLUSIONS

Both structural phase transitions and counterion (dopant) ordering have been observed in alkali-metal complexes of polyacetylene. The appearance of ordered phases and the transitions between them dominate both the conductivity and the chemical potential of the polymer complex for all doping levels $y > 0.004$. Evidence for counterion ordering is found over composition ranges which are contained within a particular structural phase. Maxima in conductivity are observed at compositions corresponding to ordered phases, e.g., at (C₄H₄)₃Na, (C₃H₃)₃Na, (C₄H₄)₄K, and (C₄H₄)₂K. As expected, increasing temperature causes a decrease in the degree of order, but no transitions to a disordered state as a function of temperature were found over the limited temperature range available to the present study, $0 < T < 75^\circ\text{C}$.

For both K⁺ and Na⁺ insertion, the initial doping was

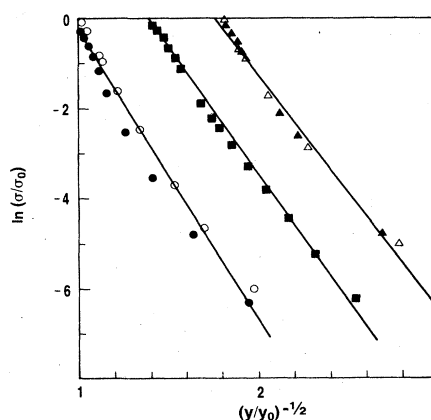


FIG. 11. Conductivity upon insertion (open symbols) and extraction (solid symbols) as a function of composition for a two-dimensional hopping model. Polyacetylene complexes contain the counterions K⁺ (circles), Na⁺ (triangles), and PF₆⁻ (squares). The abscissae of the data for each ion are successively offset by 0.4 for clarity.

found to be dominated by a discontinuous transformation from an essentially undoped phase to a heavily doped phase having $y \sim 0.06$. Over this span of compositions ($\sim 0.004 < y < 0.06$) two phases must coexist. Since these phases must be characterized by widely differing electronic conductivity, a percolation model was considered. Conductivity was found to be too rapidly varying to be explained by a percolation model obeying universal scaling laws. The observed strong dependence of conductivity on y also rules out any possible application of a model invoking macroscopic inhomogeneity of dopant distribution such as concentration near the outside surface of the film or even the surface of fibrils.

A variable-range-hopping model seems to offer the best fit to the present data. Elastic energy considerations lead to the conclusion that once a column is opened in the polymer structure, ions will tend to fill that opened channel. Conductivity will, therefore, be concentrated in the chains adjacent to the channel. Charge carriers must tunnel or hop between such conductive regions. The conductivity data are well approximated by a VRH model in the range $\sim 0.01 < y < 0.06$. The rapid variation of conductivity with doping level suggests a strong localization of carriers within conducting regions. It is also very interesting to note that the conductivity of p -type polyacetylene (PF_6^- counterions) varies in essentially the same functional way as does the n -type material (Na^+ and K^+) over the range up to 6% doping. This similarity suggests a clustering of anions to produce regions of high conductivity, even though the actual structure of the acceptor^{4,5} and donor^{5,7,16} complexes are different. Such clustering has also been observed in x-ray measurements on p -type complexes of polyacetylene with ClO_4^- .³³

The present details of the structural evolution of polyacetylene complexes can be applied to other earlier measurements of bulk properties. The dependence of magnetic susceptibility on composition has recently been measured for sodium-polyacetylene complexes formed *in situ*.³⁴ These data exhibit an abrupt rise in Pauli susceptibility (χ_p) at about $y = 0.06$. This composition corresponds roughly with the point where the rapid rise in conductivity saturates and the first plateau in electrochemical potential (i.e., the chemical potential) ends. The fact that χ_p remains low over the entire range up to $y = 0.06$ implies that the conductive phase which exists in

the two-phase region for $y < 0.06$ contains spinless carriers (solitons). The composition of this "spinless" conductive phase suggested by Fig. 3 is $y = 0.0667$, i.e., $(\text{C}_5\text{H}_5)_3\text{Na}$. Once this phase is fully formed (i.e., when the average y equals 0.0667), sodium ions will begin to be compressed into channels, and the average charge on individual chains will begin to increase. By the time the phase $(\text{C}_4\text{H}_4)_3\text{Na}$, where the conductivity reaches a maximum, has formed, the transition to carriers with spin has been completed.³⁴ Evidently, this transition to a "metallic" state occurs between doping levels equivalent to an average of one charge per 15 CH units and one per 12 CH units. This transition occurs within the phase having three polymer chains per sodium-ion column, and apparently is not directly correlated with the structural change to this phase but rather with the point where charge levels begin to exceed one in 15 on individual chains. This distance between charges roughly corresponds to estimates of the linear extent of the defect in polyacetylene.³⁵ In another recent *in situ* study,³⁶ hysteresis has been observed between electrochemical potential and spin susceptibility in sodium-doped polyacetylene. This hysteresis is to be expected on the basis of that observed between the E -versus- y curves in Figs. 3 and 4. Reference 9 provides a detailed discussion of possible mechanisms contributing to hysteresis. In essence, hysteresis is generally expected to accompany a first-order transformation from one structural phase to another [as, for example, that between nearly undoped polyacetylene and $(\text{C}_5\text{H}_5)_3\text{Na}$]. Since, as already mentioned, the work of Ref. 34 suggests that the phase $(\text{C}_5\text{H}_5)_3\text{Na}$ contains only spinless carriers, the hysteresis involved in the growth of this phase has no relation to the transition to carriers with spin which evidently occurs over a narrow range of doping³⁴ at a composition level between $(\text{C}_5\text{H}_5)_3\text{Na}$ and $(\text{C}_4\text{H}_4)_3\text{Na}$.

ACKNOWLEDGMENTS

We are pleased to acknowledge N. S. Murthy for his x-ray measurements of crystallinity, R. H. Baughman for many helpful discussions, R. L. Elsenbaumer for suggesting the synthesis of the acetylene-hexyne copolymer, and D. M. Ivory for the synthesis of polyacetylene and its copolymer with 1-hexyne.

- ¹D. MacInnes, Jr., M. A. Druy, P. A. Nigrey, D. P. Nairns, A. G. MacDiarmid, and A. J. Heeger, *J. Chem. Soc., Chem. Commun.* **1981**, 317.
- ²L. W. Shacklette, R. L. Elsenbaumer, R. R. Chance, J. M. Sowa, D. M. Ivory, G. G. Miller, and R. H. Baughman, *J. Chem. Soc., Chem. Commun.* **1982**, 361.
- ³L. W. Shacklette, R. L. Elsenbaumer, and R. H. Baughman, *J. Phys. (Paris) Colloq.* **44**, C3-559 (1983).
- ⁴R. H. Baughman, N. S. Murthy, G. G. Miller, and L. W. Shacklette, *J. Chem. Phys.* **80**, 1065 (1983).
- ⁵R. H. Baughman, N. S. Murthy, G. G. Miller, L. W. Shacklette, and R. M. Metzger, *J. Phys. (Paris) Colloq.* **44**, C3-559 (1983).
- ⁶L. W. Shacklette, N. S. Murthy, R. H. Baughman, *Mol. Cryst. Liq. Cryst.* **121**, 201 (1985).

- ⁷R. H. Baughman, L. W. Shacklette, N. S. Murthy, G. G. Miller, and R. L. Elsenbaumer, *Mol. Cryst. Liq. Cryst.* **118**, 253 (1985).
- ⁸H. Shirakawa and S. Ikeda, *Polym. J.* **2**, 3 (1971); T. Ito, H. Shirakawa, and S. Ikeda, *J. Polym. Sci. Polym. Chem. Ed.* **12**, 11 (1974).
- ⁹L. W. Shacklette, J. E. Toth, N. S. Murthy, and R. H. Baughman, *J. Electrochem. Soc.* **132**, 1529 (1985).
- ¹⁰A. H. Thompson, *Rev. Sci. Instrum.* **54**, 229 (1983).
- ¹¹J. H. Kaufman, T.-C. Chung, and A. J. Heeger, *J. Electrochem. Soc.* **131**, 2847 (1984).
- ¹²J. L. Bredas, R. Silbey, D. S. Boudreax, and R. R. Chance, *J. Am. Chem. Soc.* **105**, 6555 (1983).
- ¹³W. R. McKinnon and J. R. Dahn, *Solid State Commun.* **48**, 43 (1983).

- ¹⁴R. M. Suter, M. W. Schafer, P. M. Horn, and P. Dimon, *Phys. Rev. B* **26**, 1495 (1982).
- ¹⁵L. Landau and E. Lifshitz, *Statistical Physics* (Pergamon, Oxford, 1958).
- ¹⁶R. H. Baughman, N. S. Murthy, and G. G. Miller, *J. Chem. Phys.* **79**, 515 (1983).
- ¹⁷W. R. McKinnon, *Solid State Commun.* **40**, 343 (1981).
- ¹⁸R. Osorio and L. M. Falicov, *J. Phys. Chem. Solids* **43**, 73 (1982).
- ¹⁹A. J. Berlinsky, W. G. Unruh, W. R. McKinnon, and R. R. Haering, *Solid State Commun.* **31**, 135 (1979).
- ²⁰J. R. Dahn, D. C. Dahn, and R. R. Haering, *Solid State Commun.* **42**, 179 (1982).
- ²¹H. Eckhardt, L. W. Shacklette, J. S. Szobota, and R. H. Baughman, *Mol. Cryst. Liq. Cryst.* **117**, 401 (1985).
- ²²Y. Tomkiewicz, T. D. Schultz, H. B. Broom, T. C. Clarke, and G. B. Street, *Phys. Rev. Lett.* **43**, 1532 (1979).
- ²³D. M. Hoffman, D. B. Tanner, A. J. Epstein, and H. W. Gibson, *Mol. Cryst. Liq. Cryst.* **83**, 1175 (1982).
- ²⁴*Percolation Structures and Processes*, Annals of the Israel Physical Society (Hilger, Bristol, 1983), Vol. 5.
- ²⁵C. Mathis and B. Francois, *Synth. Met.* **8**, 347 (1984).
- ²⁶G. E. Pike and C. H. Seager, *Phys. Rev. B* **10**, 1421 (1974).
- ²⁷N. F. Mott and E. A. Davis, *Electronic Processes in Non-Crystalline Materials*, 2nd ed. (Clarendon, Oxford, 1979).
- ²⁸V. Ambegaokar, B. I. Halperin, and J. S. Langer, *Phys. Rev. B* **4**, 2612 (1971).
- ²⁹R. Colson and P. Nagels, *J. Non-Cryst. Solids* **35& 36**, 129 (1980).
- ³⁰A. J. Epstein, H. Rommelmann, R. Bigelow, H. W. Gibson, D. M. Hoffman, and D. B. Tanner, *Phys. Rev. Lett.* **50**, 1866 (1983).
- ³¹J. Kanicki, E. VanderDonckt, and S. Boue, *J. Chem. Soc. Faraday Trans. 2* **77**, 2157 (1981).
- ³²H. Overhof, *Festkörperprobleme XVI*, edited by J. Treusch (Pergamon/Vieweg, Braunschweig, 1976), p. 239.
- ³³J. P. Pouget, J. C. Pouxviel, P. Robin, R. Comes, D. Begin, D. Billaud, A. Feldblum, H. W. Gibson, and A. J. Epstein, *Mol. Cryst. Liq. Cryst.* **117**, 75 (1985).
- ³⁴T.-C. Chung, F. Moraes, J. D. Flood, and A. J. Heeger, *Phys. Rev. B* **29**, 2341 (1984).
- ³⁵D. S. Boudreaux, R. R. Chance, J. L. Bredas, and R. Silbey, *Phys. Rev. B* **18**, 6927 (1983), and references therein.
- ³⁶J. Chen, T.-C. Chung, F. Moraes, and A. J. Heeger, *Solid State Commun.* **53**, 757 (1985).